

## Dielectric and microwave properties of elastomer composites loaded with carbon–silica hybrid fillers

Ahmed A. Al-Ghamdi,<sup>1</sup> Omar A. Al-Hartomy,<sup>1</sup> Falleh R. Al-Solamy,<sup>2</sup> Nikolay Dishovsky,<sup>3</sup> Mihail Mihaylov,<sup>3</sup> Petrunka Malinova,<sup>3</sup> Nikolay Atanasov<sup>4,5</sup>

<sup>1</sup>Department of Physics, Faculty of Science, King Abdulaziz University, 21589 Jeddah, Saudi Arabia

<sup>2</sup>Department of Mathematics, Faculty of Science, King Abdulaziz University, 21589 Jeddah, Saudi Arabia

<sup>3</sup>Department of Polymer Engineering, University of Chemical Technology and Metallurgy, 1756 Sofia, Bulgaria

<sup>4</sup>Department of Wireless Communications and Broadcasting, Graduate School of Telecommunications, 1700 Sofia, Bulgaria

<sup>5</sup>Department of Communication and Computer Engineering, Faculty of Engineering, Neofit Rilski South-West University of Blagoevgrad, 2700 Blagoevgrad, Bulgaria

Correspondence to: N. Dishovsky (E-mail: dishov@uctm.edu)

**ABSTRACT:** In this study, we investigated the influence of carbon–silica dual-phase fillers on the dielectric and microwave properties of natural-rubber-based composites determined in the frequency range from 1 to 12 GHz. The fillers were prepared by the impregnation of two types of carbon black with various silicasol amounts. As the results show, the fillers affected both the dielectric and microwave properties of the obtained composites. The higher the quantity of the dielectric phase (silica) in the hybrid filler was, the lower the real part of the permittivity of the composites was. This caused changes in the total, reflective, and absorptive shielding effectivenesses of the latter and their reflection and attenuation coefficients. © 2015 Wiley Periodicals, Inc. *J. Appl. Polym. Sci.* **2016**, *133*, 42978.

**KEYWORDS:** composites; conducting polymers; dielectric properties; rubber

Received 1 July 2015; accepted 23 September 2015

DOI: 10.1002/app.42978

### INTRODUCTION

Elastomer-based materials with active performances against electromagnetic waves find two main applications as shields (whose mechanism consists of reflection) and microwave absorbers.

Elastomer electromagnetic interference (EMI) shielding materials are particularly important for protecting biosystems and navigation and telecommunication devices from harmful and undesired electromagnetic waves radiated by similar equipment located in a close vicinity.<sup>1–5</sup> An effective reflecting shield should possess mobile charge carriers interacting with the unwanted electromagnetic waves. Therefore, there is a tendency for those shields to be electroconductive, but they are not required to possess a high conductivity.<sup>6</sup> The greater part of virgin elastomers are dielectrics and are entirely transparent to electromagnetic radiation; that is, their EMI shielding effectiveness (SE) is practically zero. That is why good EMI shielding materials can be obtained only via the creation of conductive pathways by the introduction of electroconductive fillers apt to form chainlike structures in the dielectric rubber matrix.<sup>5,7</sup> This was confirmed by the investigations of Rahaman *et al.*<sup>5</sup> They

established that at the same degree of filling, the elastomers composed of electroconductive Printex carbon black, whose particles were more prone to forming such structures, had conductivity and EMI SE values higher than those of composites filled with Conductex, whose particles were less prone to aggregation and agglomeration.

Elastomer-based microwave absorbers find applications mostly in the manufacturing of rubber radar-absorbing materials, in reducing the radar cross section of objects, and so on.<sup>8–10</sup> As is known, the main principles for the development of elastomer-based microwave absorbers are the determination of a suitable dielectric rubber matrix and a filler or a system of fillers possessing high dielectric and/or magnetic loss values. The crucial factor for obtaining good microwave absorbers is the ability of the dielectric matrix or any other phase to completely isolate the particles of the conducting filler, that is, so its particles have fewer contacts with each other.<sup>11</sup> In most cases, this requires the use of the filler in small amounts; this has a negative effect on the mechanical properties of the rubber composites.

In our previous article,<sup>12</sup> we reported on the production of four sorts of carbon–silica dual-phase fillers via the impregnation of

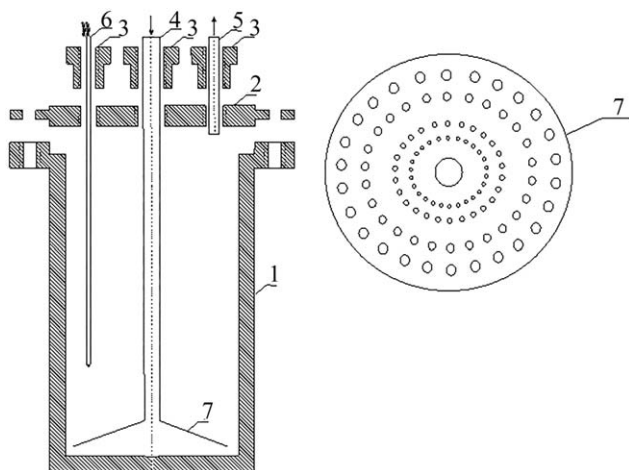


**Figure 1.** Design of the reactor used: (1) reactor vessel, (2) top (sealing flange), (3) sealing nuts, (4) gas inlet, (5) gas outlet, (6) thermocouple, and (7) Buchner funnel.

two completely different types of carbon black with various amounts of silicasol. The textural characteristics and STEM-EDS (Scanning Transmission Electron Microscopy - Energy Dispersive X-ray Spectroscopy) analysis of the hybrid fillers obtained showed a good interpenetration of the two phases (silica and carbon black) and the isolation of carbon black particles by the silica particles. The fillers thus prepared did not significantly change the curing and mechanical characteristics of the vulcanizates comprising them but improved their thermal aging resistance. The results reveal impregnation with silicasol to be a perspective method for preparing hybrid fillers. The method allows easy control over the quantitative ratio of the two phases and the mode and domain of their distribution throughout the hybrid fillers. This is a prerequisite for the targeted modification both the mechanical and microwave properties of the elastomer composites comprising those fillers.

It is a fact that a good number of authors have studied the microwave properties of composites composed of silica and carbon materials in various forms.<sup>13,14</sup> That is why it is worth investigating the dielectric and microwave properties of natural-rubber-based composites composed of hybrid carbon-silica fillers prepared by the impregnation of conventional carbon black with silicasol.

According to our working hypothesis, if the silica (dielectric) phase is located over the surface or penetrates the inner domains of carbon black aggregates (conductive phase), it should isolate them and restrict their interaction. That will allow the use of larger filler amounts and, hence, open opportunities to obtain elastomer composites with good mechanical and microwave properties suitable for producing microwave-absorbing materials.

## EXPERIMENTAL

### Materials

Natural rubber SVR 10, supplied by Hong Thanh Rubber Pty., Ltd., was used as the polymer matrix. The other ingredients, including zinc oxide (ZnO), stearic acid, *N-tert*-butyl-2-benzo-

thiazole sulfenamide, and sulfur, were commercial grade and were used without further purification.

### Hybrid Filler Preparation

Industrial furnace carbon black type PM-15 (produced in Russia with characteristics close to those of carbon black type N 776) and carbon black type PM-75 (produced in Russia with characteristics close to those of carbon black type N 330) were used as substrates. Silicasol (containing 40% of silica, pH = 9, density = 1.3 g/cm<sup>3</sup>) was chosen as an impregnating agent because of our idea to obtain carbon-silica dual-phase fillers. The choice of the two fillers was determined by the great difference in their main characteristics: specific surface area, particle size, oil absorption number, iodine adsorption, and so on. Both fillers were impregnated with silicasol, equivalent to 3 and 7% silica, respectively. The obtained hybrid fillers were denoted as ICSF-15-3, ICSF-15-7, ICSF-75-3, and ICSF-75-7. The letters denote hybrid fillers having two phases (carbon black and silica) obtained by an impregnation technology. The digits following the letters denote the specific surface area of the carbon black used as a hybrid filler substrate, and the last digit denotes the percentage of silica used.

The hybrid fillers were prepared via impregnation according to the following procedure:

1. The needed amount of silicasol (estimated so that the impregnation solution was composed of 3 or 7% silica) was diluted in 400 mL of distilled water. A ball mill was loaded with 100 g of carbon black, and the silicasol solution was poured over it. The impregnation and homogenization were run for 2 h.
2. After the impregnation, the filler was dried, first at 50°C for 30 min and then at 200°C for 2 h. After that, it was ground in a ball mill for 2 h.
3. The dry ground filler was transferred into a customized reactor (Figure 1), where it was thermally treated at 440°C under a 10<sup>-2</sup>-mmHg vacuum for 2 h. The reactor was designed so that the thermal activation could be run *in vacuo* at higher temperatures without the carbon material being spoiled.
4. Being removed from the reactor, the sample was again ground in the ball mill for 2 h.

The design of the reactor used is presented in Figure 1.

### Preparation of the Rubber Composites

The rubber compounds studied were prepared on a two-roll laboratory mill (roll Length × Diameter = 320 × 160 mm). Table I presents the compositions of the studied rubber compounds.

The vulcanization of the natural-rubber-based compounds was carried out on an electrically heated hydraulic press with a special homemade mold at 150°C and 10 MPa.

### Measurements

**Dielectric Property Measurements.** *Complex permittivity* ( $\epsilon$ ). The determination of  $\epsilon$  [ $\epsilon = \epsilon' - j\epsilon''$ , where  $\epsilon''$  is the imaginary part of the complex permittivity (loss factor)] was carried out by the resonance method on the basis of the cavity

**Table I.** Compositions of the Investigated Rubber Compounds

	NR 1	NR 2	NR 3	NR 4	NR 5	NR 6
Natural rubber SVR 10	100.0	100.0	100.0	100.0	100.0	100.0
ZnO	3.0	3.0	3.0	3.0	3.0	3.0
Stearic acid	2.0	2.0	2.0	2.0	2.0	2.0
Carbon black PM-15	70.0	—	—	—	—	—
Carbon black PM-75	—	70.0	—	—	—	—
ICSF-15-3	—	—	70.0	—	—	—
ICSF-15-7	—	—	—	70.0	—	—
ICSF-75-3	—	—	—	—	70.0	—
ICSF-75-7	—	—	—	—	—	70.0
TBBS	1.5	1.5	1.5	1.5	1.5	1.5
Sulfur	2.0	2.0	2.0	2.0	2.0	2.0

TBBS, *N-tert-butyl-2-benzothiazole sulfenamide*.

perturbation technique. The resonance frequency of an empty cavity resonator ( $f_r$ ) was also measured. After that, the sample material was placed into the resonator and the shift in resonance frequency ( $f_e$ ) was measured. The real part of the permittivity [dielectric constant ( $\epsilon_r'$ )] was calculated from  $f_e$  and the cavity and sample cross sections ( $S_r$  and  $S_e$ , respectively):

$$\epsilon_r' = \frac{S_r}{2S_e} \times \frac{f_r - f_e}{f_r} \quad (1)$$

The sample had the form of a disc with a diameter of 11 mm and a thickness of about 1.5 mm. It was placed at the spot of the maximum electric field of the cavity. Because the thickness of the sample was not equal to the height of the resonator, a dielectric occurred with an equivalent permittivity ( $\epsilon_e$ ) at the spot of its location. The parameter was determined by eq. (1), and instead of  $\epsilon_r'$ , it was saved as  $\epsilon_e$ . Then,  $\epsilon_r'$  was determined as follows:

$$\epsilon_r' = \epsilon_e(k+1) - k \quad (\Delta \ll l) \quad (2)$$

where  $k = l/\Delta$ ,  $k$  is the coefficient,  $\Delta$  is the thickness of the sample, and  $l$  is the distance from the disk to the top of the resonator.

$\epsilon''$ .  $\epsilon''$  was calculated from the quality factors of the cavity with a sample ( $Q_e$ ) and without a sample ( $Q_r$ ):

$$\epsilon'' = \frac{1}{4\epsilon_r'} \times \frac{S_r}{S_e} \left( \frac{1}{Q_e} - \frac{1}{Q_r} \right) \quad (3)$$

The measurement setup used several generators for the whole range (HP686A and G4-79 to 82), frequency meters (H 532A and FS-54), and a cavity resonator (Figure 2). The dielectric properties were measured within the frequency range from 1 to 12 GHz.

**Electrical Property Measurements.** *Volume resistivity* ( $\rho_v$ ).  $\rho_v$  ( $\Omega$  m) of the studied composites was measured with two electrodes (two-terminal method) and calculated by the following equation:

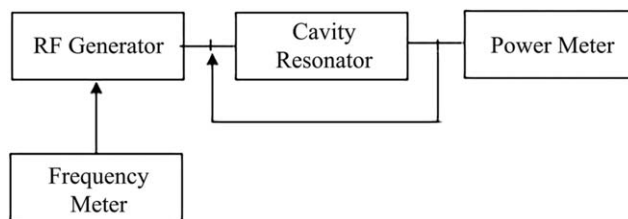


**Figure 2.** Scheme of the equipment for measuring the dielectric properties. (RF Generator - Radiofrequency Generator).

$$\rho_v = R_v \frac{S}{h} \quad (4)$$

where  $R_v$  is the Ohmic resistance between the electrodes,  $h$  is the sample thickness between the electrodes (m), and  $S$  is the cross-sectional area of the measuring electrode ( $m^2$ ).

A Wheatstone bridge was used to measure the resistance.

**Surface resistivity** ( $\rho_s$ ). The  $\rho_s$  values of the samples were calculated with the following equation:

$$\rho_s = 100R_s \quad (5)$$

where  $R_s$  is the resistivity ( $\Omega$ ).

**Microwave Property Measurements.** Figure 3 presents the mechanism of a composite's interaction with an electromagnetic wave with incident power ( $P_I$ ). A fraction of the power of the wave reflects back by the surface of the material [reflected power ( $P_R$ )]. Another fraction passes through the material while being absorbed by it and converted into heat [absorbed power ( $P_A$ )], whereas the remainder gets transmitted [transmitted power ( $P_T$ )].

The total shielding effectiveness ( $SE_T$ ) was defined as the ratio between  $P_I$  on the sample and  $P_T$  in accordance with eq. (6)<sup>15-17</sup>:

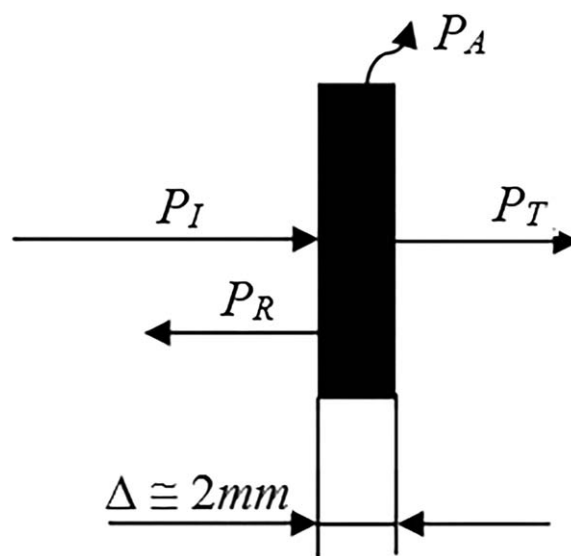


**Figure 3.** Schematic presentation of a shielding material interacting with an electromagnetic wave of  $P_I$ .

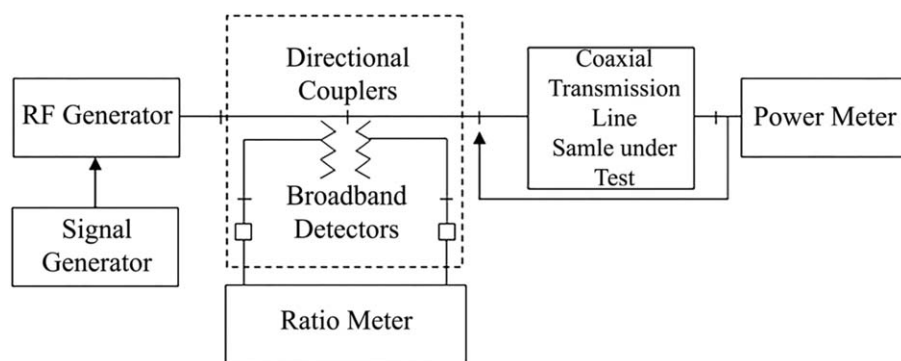


**Figure 4.** Apparatus for measuring the microwave properties. (RF Generator - Radiofrequency Generator).

$$SE = 10 \log \frac{P_I}{P_T} \quad (6)$$

$SE_T$  (dB) and the reflective shielding effectiveness ( $SE_R$ ) of the sample surface (dB) were determined by eqs. (7) and (8)<sup>18–21</sup>:

$$SE_T = -10 \lg T \quad (7)$$

Where

$$T = |P_T/P_I| = |S_{21}|^2$$

$$SE_R = -10 \lg(1-R) \quad (8)$$

Where

$$R = |P_R/P_I| = |S_{11}|^2$$

where  $T$  is the transmittance and  $R$  is the reflection.  $S_{11}$  and  $S_{21}$  are complex scattering parameters or  $S$  parameters.  $S_{11}$  corresponds to the reflection coefficient, and  $S_{21}$  corresponds to the transmission coefficient.

The absorptive shielding effectiveness ( $SE_A$ ) was calculated as the difference between eq. (7) and eq. (8), as shown in eq. (9):

$$SE_A = SE_T - SE_R \quad (9)$$

Figure 4 presents the schematic diagram of the measurement system for EMI SE in a broadband frequency range. The experimental setup consisted of a coaxial reflectometer (Narda model 4222-16 coaxial directional couplers; Narda FSCM 998999 model 4503A detectors, with  $P_I$  separated from  $P_R$  in the transmission line); an HP model 416A ratio meter, which calculated and displayed the amplitude of the reflection coefficient; a series of generators (G4-37A, G4-79 to G4-82, and HP 68A), which provided radiofrequencies in the range from 1 to 12 GHz; a BM492 signal generator, which released a modulating signal at 1 kHz that was directed toward the radiofrequency generator; an Orion type E2M coaxial transmission line for frequencies from 1 to 5 GHz; an APC-7 mm coaxial measuring line for frequencies from 6 to 12 GHz; and an HP 432A power meter. The cutoff frequencies for the coaxial measuring lines were determined by formulas presented in the literature.<sup>22,23</sup> The sample holder, reflectometer setup, and radiofrequency generator were connected with a rugged phase stable cable N9910X-810 Agilent and through the connectors without interference from other components.

The ratio meter was calibrated before we carried out the actual measurements. A calibrating open-short-load procedure was applied with Agilent N9330 and Agilent 1250 calibration kits.

The measurements of  $P_I$ ,  $P_T$ , and reflection coefficient were performed with the following procedure:

1. Preparation of the measuring system.
2. Calibration of the system with calibration kits to eliminate systematic errors from the proper measurement.
3. Preparation of the samples through the cutting out of pieces from the obtained vulcanized materials having dimensions as follows:
  - External diameter of 20 mm and internal diameter of 7 mm when a coaxial transmission line Orion E2M was used.
  - External diameter of 7 mm and internal diameter of 3 mm when a coaxial measuring line APC-7 mm was used.
4. Measurements to determine the modulus of the reflection coefficient ( $|\Gamma|$ ) with
  - Standard load of type Agilent 1250 connected in the position of the coaxial line.
  - Blank coaxial line with a standard load at the end (Agilent N9330 calibrating kit of tools).
5. Measurement of  $P_I$ .
6. Measurement of the reflection coefficient and  $P_T$  by careful placement of the cut-out sample inside the coaxial line.
7. Measurement of the reflection coefficient and  $P_T$  for confirming the correctness of the measurements done by the placement of the cut-out standard material [polytetrafluoroethylene (PTFE); thickness load = 1 mm] into the coaxial line.

The measurements were carried out at room temperature from 19 up to 24°C and with  $P_I$  at the inlet of the coaxial measuring line varied from 800 up to 1300  $\mu$ W within a frequency range of 1–12 GHz.

## RESULTS AND DISCUSSION

### Dielectric Properties

Figure 5 presents the frequency dependence of  $\epsilon_r'$  of the studied natural-rubber-based composites comprising the obtained hybrid fillers.

As shown in Figure 5, the dependence was of a well-pronounced resonance character. The highest values of  $\epsilon_r'$  for all

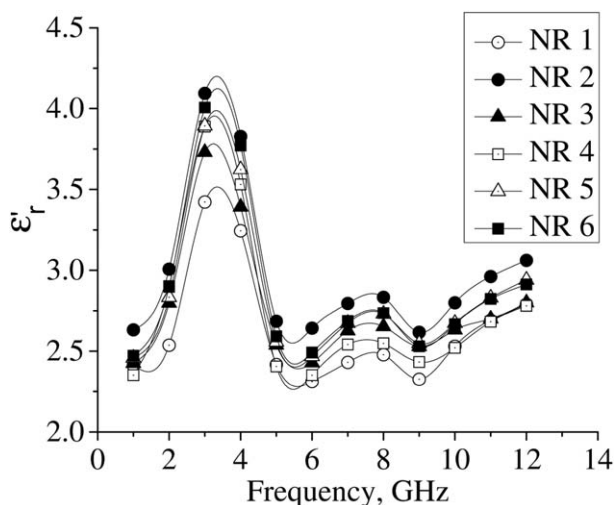


Figure 5. Frequency dependence of  $\epsilon_r'$  for the studied composites.

of the studied composites were observed at about 3 GHz. In the range between 5 and 12 GHz, there were no significant changes in the  $\epsilon_r'$  values; this depended on the frequency. The NR 2 composite filled with PM-75 carbon black possessed the highest values throughout the entire frequency range studied. The NR 1 composite filled with PM-15 carbon black had the lowest values of  $\epsilon_r'$ . This was due to the difference in the particle size of the two fillers and their ability to form chain structures (conductive pathways).<sup>12</sup> The smaller size of the PM-75 carbon black particles and their aptitude to form chain structures favored the creation of electrical (conductive) pathways. Hence, the interfacial polarization resulting from the inhomogeneity introduced by the filler particles became easier, and consequently,  $\epsilon_r'$  increased. The higher values of  $\epsilon_r'$  showed the easily accomplished molecular polarization.<sup>24</sup>

The  $\epsilon_r'$  values of the NR 5 and NR 6 composites comprising the hybrid fillers ICSF-75-3 and ICSF-75-7 and prepared by impregnation of conventional PM-75 carbon black with silicasol were slightly lower than those of the NR 2 composite filled with the substrate PM-75 carbon black. The penetration of the silica phase among the chain structures of carbon black and their isolation hindered the creation of conductive pathways. That hindered the molecular polarization; hence,  $\epsilon_r'$  of the obtained composites was lower. The NR 1 composite filled with the conventional PM-15 carbon black and composites NR 3 and NR 4 comprising the hybrid fillers based on conventional PM-15 carbon black did not share the previously mentioned tendency because the interpenetration of the two phases was less pronounced.<sup>12</sup>

As shown in Figure 5, in all cases, the  $\epsilon_r'$  values were generally rather low. This was due to the fact that the carbon black used was of very low electroconductivity. On the other hand, the polymer matrix was nonpolar and crystallizing; this hindered the molecular polarization.<sup>25,26</sup>

The frequency dependence of  $\epsilon''$  of the studied composites is presented in Figure 6.

Figure 6 shows  $\epsilon''$  to be a parameter that was very sensitive to frequency changes and to the type of filler used. In the fre-

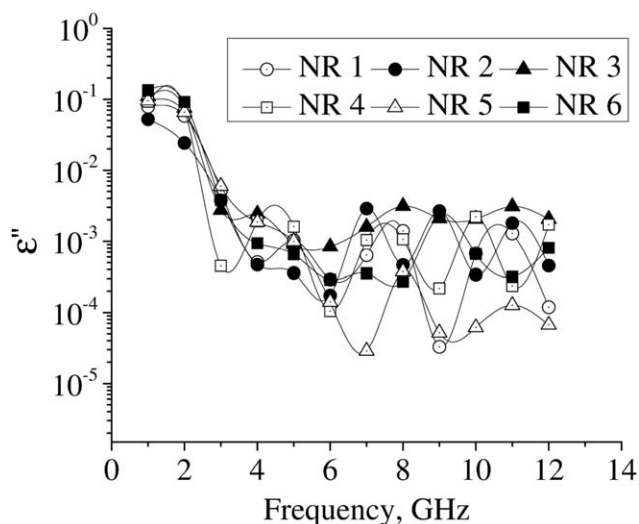


Figure 6. Frequency dependence of  $\epsilon_r''$  for the studied composites.

quency range 1–5 GHz,  $\epsilon''$  decreased with increasing frequency, whereas in the range 5–12 GHz, the parameter was of a well-pronounced resonance character.

#### Electrical Properties

Table II presents the values of  $\rho_v$  and  $\rho_s$  for the studied composites. The obtained results are in full agreement with the dielectric properties data. As Table II shows, the  $\rho_v$  values of the NR 1 composite, which was filled with conventional PM-15 carbon black, and those of the NR 3 and NR 4 composites comprising the PM-15-based hybrid fillers varied in the range from  $3.0 \times 10^{12}$  to  $1.2 \times 10^{13} \Omega \text{ m}$ . In this case, the studied composites were attributed as dielectrics. The  $\rho_v$  values of the NR 2 composite filled with PM-75 carbon black and the NR 5 and NR 6 composites comprising the PM-75-based hybrid fillers were much lower and varied in the range from  $2.2 \times 10^3$  to  $3.8 \times 10^3 \Omega \text{ m}$ ; that is, those composites were semiconductors. As we mentioned previously, this was due to the difference in the particles size of the two types of carbon black. The smaller size of the PM-75 carbon black particles and their aptitude to form chain structures favored the creation of conductive pathways. Therefore, the  $\rho_v$  values of the studied composites were lower, whereas their conductivity was higher. According to Table II, in all cases, the  $\rho_v$  and  $\rho_s$  values of the composites comprising the investigated hybrid fillers increased with increasing silica content in the latter; that is, their conductivity decreased. This was due to the silica phase penetration among the chainlike structures of

Table II.  $\rho_v$  and  $\rho_s$  Values of the Studied Composites

	$\rho_v$ ( $\Omega \text{ m}$ )	$\rho_s$ ( $\Omega$ )
NR 1	$3.0 \times 10^{12}$	$5.1 \times 10^{14}$
NR 2	$2.2 \times 10^3$	$2.3 \times 10^6$
NR 3	$4.2 \times 10^{12}$	$5.9 \times 10^{14}$
NR 4	$1.2 \times 10^{13}$	$6.5 \times 10^{14}$
NR 5	$3.0 \times 10^3$	$3.4 \times 10^6$
NR 6	$3.8 \times 10^3$	$6.0 \times 10^6$

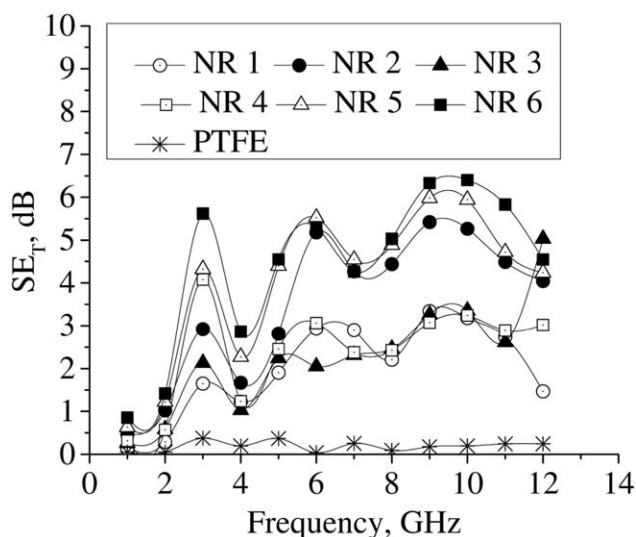


Figure 7. Frequency dependence of  $SE_T$  of the studied composites.

carbon black. Thus, the dielectric phase insulated the conductive one, and the formation of conductive pathways was hindered, and this resulted in a lower conductivity of the composite. The obtained results were in full agreement with our working hypothesis.

#### Microwave Properties

Figures 7–9 present the frequency dependencies of  $SE_T$ ,  $SE_R$ , and  $SE_A$  for the studied composites and for the control sample (PTFE).

As shown in Figure 7, the elastomer NR 2 composite filled with PM-75 carbon black and the NR 5 and NR 6 composites comprising the hybrid fillers based on PM-75 carbon black had the highest values of  $SE_T$ . The NR 1 composite filled with PM-15 carbon black and the NR 3 and NR 4 composites, whose hybrid fillers were based on PM-15 possessed  $SE_T$  values that were lower than those of the composites comprising PM-75. Obviously, there was a tendency toward increasing  $SE_T$  values with

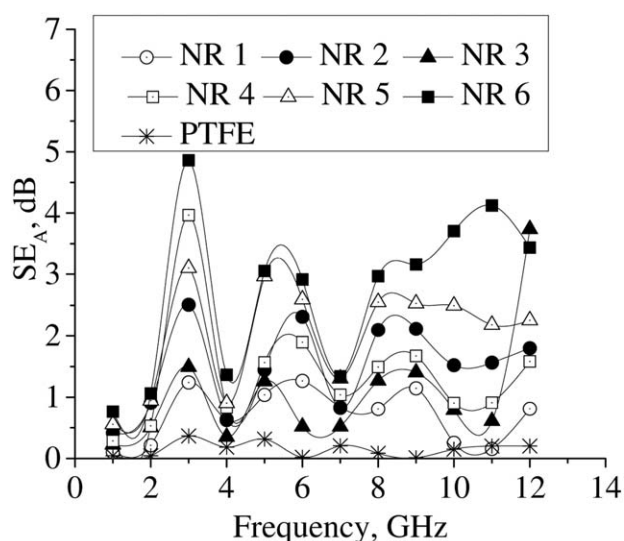


Figure 9. Frequency dependence of  $SE_A$  of the studied composites.

increasing silica amount in the hybrid fillers. That was explained by the interpenetration of the two phases, and this caused the changes occurring in  $SE_R$  and  $SE_A$  (Figures 8 and 9). Frequency changes also affected the  $SE_T$  values of the studied composites. As Figure 7 shows, at frequencies of 1 and 2 GHz, all of the samples were transparent to electromagnetic waves, and their  $SE_T$  values tended to zero. In the frequency range from 2 to 12 GHz, the dependency was of a resonance character. Throughout the entire frequency range, the control sample (PTFE) did not exhibit shielding properties; that is, its  $SE_T$  values tended to zero. This justified the correctness of the experiment that we carried out.

As shown in Figure 8, the elastomer NR 2 composite filled with conventional PM-75 carbon black had the highest  $SE_R$  values. The NR 5 and NR 6 composites comprising hybrid fillers possessed lower  $SE_R$  values. Moreover, there was a tendency toward decreasing  $SE_R$  values of the composites with increasing amount

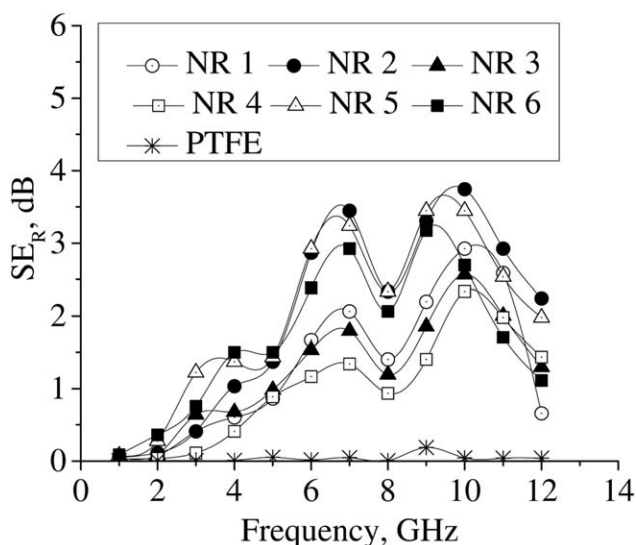


Figure 8. Frequency dependence of  $SE_R$  of the studied composites.

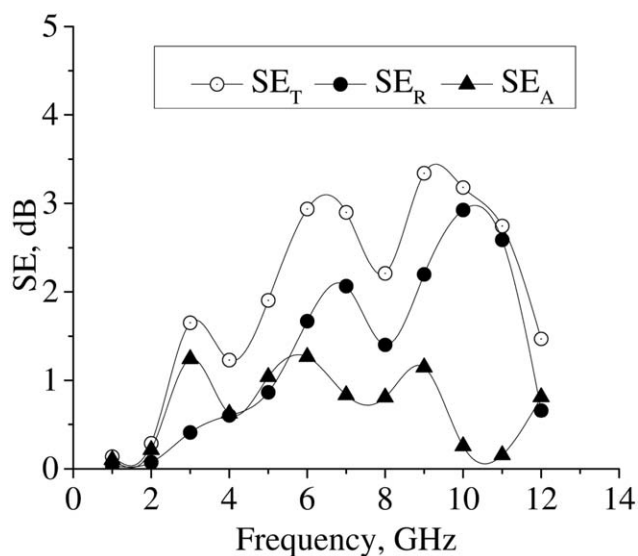


Figure 10. Frequency dependence of  $SE_T$ ,  $SE_R$ , and  $SE_A$  of sample NR 1.

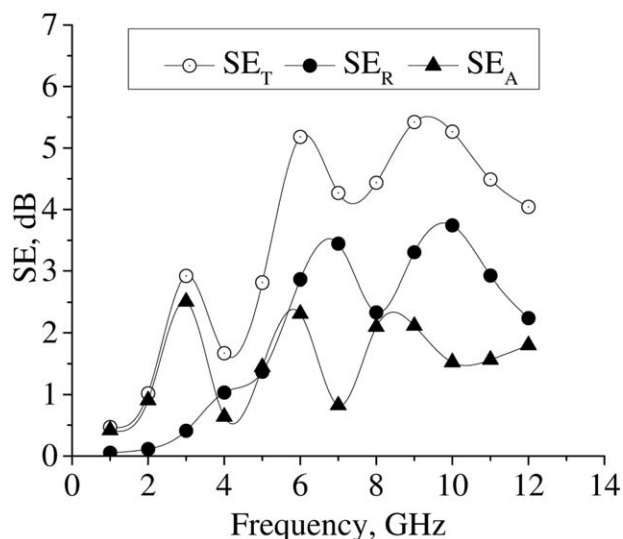


Figure 11. Frequency dependence of  $SE_T$ ,  $SE_R$ , and  $SE_A$  of sample NR 2.

of the filler's second phase (silica). The tendency was also observed in the case of the NR 1 composite filled with conventional PM-15 carbon black and in the case of the NR 3 and NR 4 composites comprising hybrid fillers having PM-15 carbon black as a substrate. However, the  $SE_R$  values in those cases were lower than the  $SE_R$  values of the composites comprising PM-75 carbon black and PM-75-based hybrid fillers. The figure shows that the frequency dependence of  $SE_R$  was of a resonance character, whereas the lower values of PTFE (absolutely transparent to microwaves) tending to zero justified the correctness of the experiment that we carried out.

As shown in Figure 9,  $SE_A$  of the studied composites was the reverse of  $SE_R$ . The composites comprising hybrid fillers possessed the highest  $SE_A$  values, which decreased with decreasing silica amount in the fillers. In this case, the NR 2 composite comprising PM-75 carbon black and the NR 5 and NR 6 com-

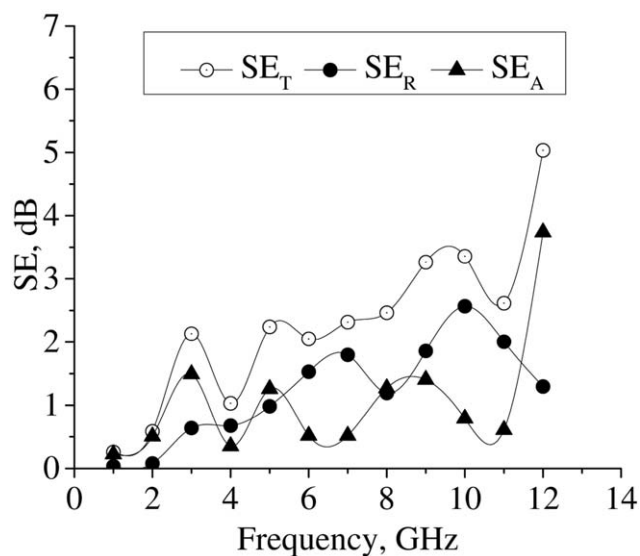


Figure 12. Frequency dependence of  $SE_T$ ,  $SE_R$ , and  $SE_A$  of sample NR 3.

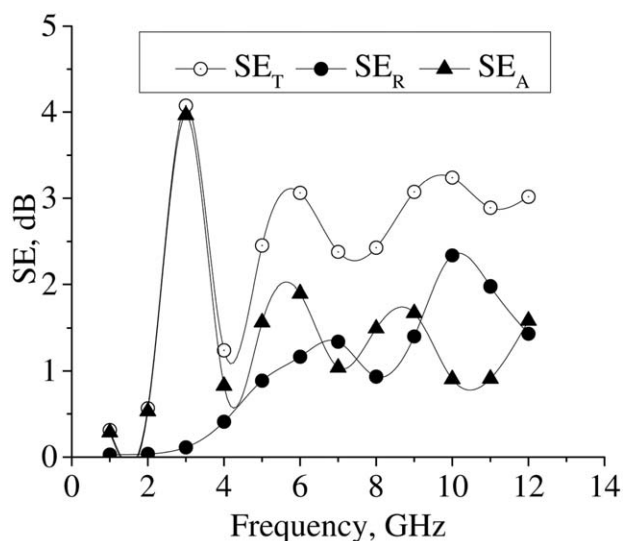


Figure 13. Frequency dependence of  $SE_T$ ,  $SE_R$ , and  $SE_A$  of sample NR 4.

posites comprising hybrid fillers with PM-75 carbon black as a substrate also exhibited the best properties.

For better comprehension of the changes in  $SE_T$ ,  $SE_R$ , and  $SE_A$  values, Figures 10–15 present their frequency dependence separately for each composite.

As Figures 10 and 11 show, for the NR 1 and NR 2 composites filled with unmodified conventional carbon black,  $SE_A$  predominated in the range from 1 to 5 GHz; that is,  $SE_T$  was determined by  $SE_A$ . In the range from 5 to 12 GHz, however,  $SE_R$  dominated. Obviously, the use of hybrid fillers led to significant changes in this respect (Figures 12–15). Those changes were most pronounced in the case of composites comprising the hybrid filler obtained by the impregnation of the conventional PM-75 carbon black with silicasol. As shown in Figure 15, in the entire frequency range,  $SE_A$  predominated in  $SE_T$  of the composite comprising a hybrid filler prepared from PM-75 carbon black with a 7% content of silica. This was due to the

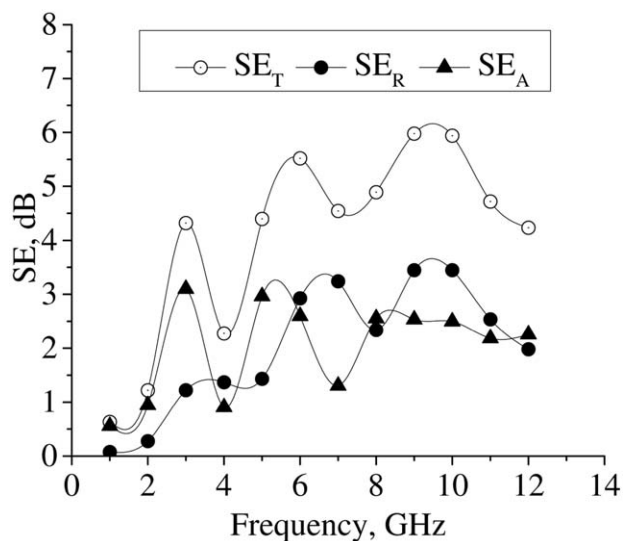


Figure 14. Frequency dependence of  $SE_T$ ,  $SE_R$ , and  $SE_A$  of sample NR 5.

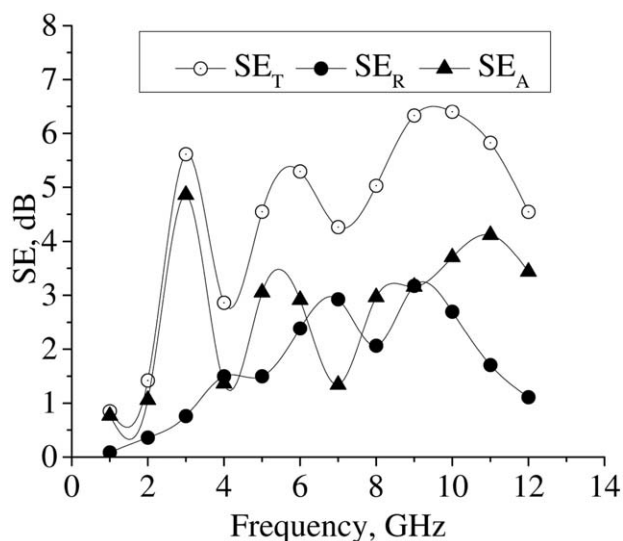


Figure 15. Frequency dependence of  $SE_T$ ,  $SE_R$ , and  $SE_A$  of sample NR 6.

isolation of the conductive carbon black phase by the dielectric silica phase, which hindered the formation of conductive pathways.

The values for  $SE_T$ ,  $SE_R$ , and  $SE_A$  of the NR 2 composite filled with conventional PM-75 carbon black and the NR 5 and NR 6 composites comprising hybrid fillers with PM-75 carbon black as a substrate were higher than those of the NR 1, NR 3, and NR 4 composites comprising fillers based on PM-15 carbon black. This was due to the difference in the particles size of the fillers and their aptitude to form secondary (chain) structures. The particle interaction in the unmodified fillers was better. Hence, the conductive pathways in the elastomer composites were created more easily. This determined the higher  $\epsilon_r'$  values of those composites and the domination of  $SE_R$  in their  $SE_T$  values. The introduction of a certain silica amount via carbon black impregnation with silicasol insulated the particles of the former and obstructed the creation of conductive pathways in it. Therefore, the composites comprising the hybrid fillers had a lower  $\epsilon_r'$ , and  $SE_A$  predominated in their  $SE_T$ 's.

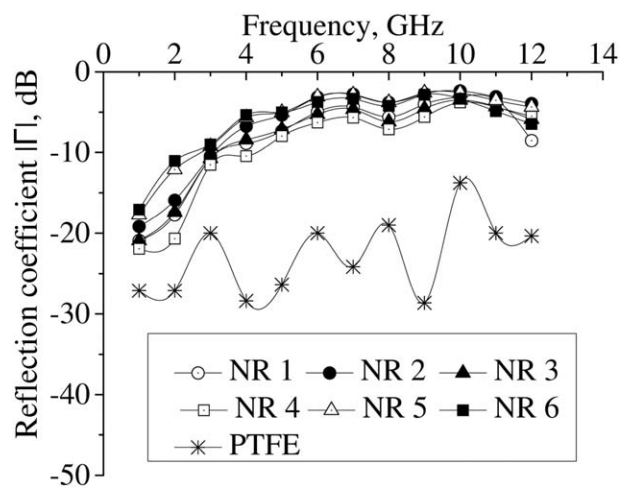


Figure 16. Frequency dependence of  $|\Gamma|$  in a logarithmic scale.

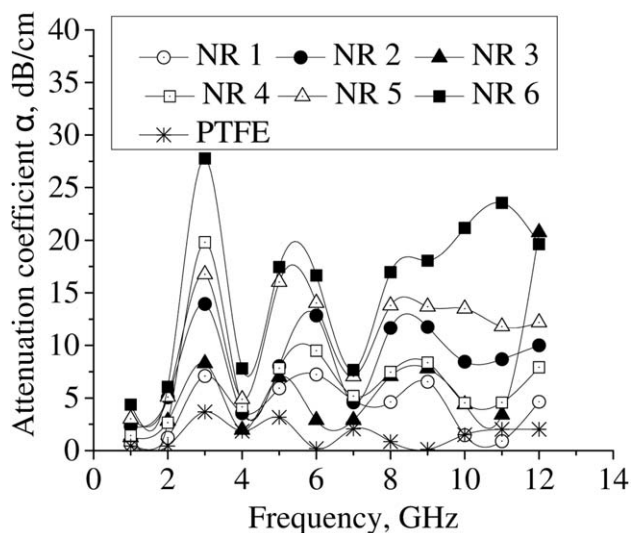


Figure 17. Frequency dependence of the attenuation coefficient.

Figures 16 and 17 present the frequency dependences of the reflection and the attenuation coefficients for the studied composites.

As shown in Figures 16 and 17, the data about the reflection and attenuation coefficients in the studied frequency range were analogous to those about  $SE_R$  and  $SE_A$  (Figures 8 and 9). Obviously, in the 1–7 GHz range,  $|\Gamma|$  for all materials increased almost linearly (monotonously), whereas in the 10–12-GHz range,  $|\Gamma|$  decreased. The electromagnetic attenuation was best pronounced for the composites comprising hybrid fillers obtained via the impregnation of conventional carbon black with silicasol and, particularly, for those composites whose fillers were based on PM-75 carbon black.

The obtained results show that the use of dual-phase fillers of different ratios of the conductive and dielectric phase furnished the easy control and tailoring the microwave properties of electromagnetic composites. On the other hand, the impregnation technology is an unsophisticated method for controlling the quantitative ratio of the two phases in such fillers.

## CONCLUSIONS

The study revealed the effect that the hybrid fillers prepared by the impregnation of two types of carbon black with various silicasol amounts had upon the dielectric and microwave properties of natural-rubber-based composites as determined in the frequency range from 1 to 12 GHz. It was established that the fillers used affected both the dielectric and microwave properties of the obtained composites. The higher the quantity of the dielectric phase (silica) in the hybrid filler was, the lower  $\epsilon_r'$  of the composites was. The fact shows evidence of the lower conductivity of those composites, which was confirmed by their  $\rho_v$  and  $\rho_s$  values. As a result, the SE of the composites and their reflection and attenuation coefficients changed.  $SE_A$  for the composites filled with unmodified conventional carbon black dominated in the frequency range from 1 to 5 GHz, whereas in the range from 5 to 12 GHz,  $SE_R$  predominated. In the case of the composites comprising hybrid fillers of higher silica amounts,  $SE_A$  predominated in the entire frequency range studied. That was mainly due to the interpenetration of the two

filler phases and the insulation of the conductive carbon phase by the dielectric silica one. The data about the reflection and attenuation coefficients in the frequency range studied were analogous to those of  $SE_R$  and  $SE_A$ . The electromagnetic attenuation was best pronounced in the case of the composites comprising fillers prepared by the impregnation of conventional carbon black with silicasol and particularly of those prepared with PM-75 carbon black as a substrate.

The obtained results show that with the dual-phase fillers of various conductive–dielectric phase ratios, one could easily control and tailor the microwave properties of the elastomer composites. On the other hand, the impregnation technology is an easy method for establishing control over the quantitative ratio of the two phases in the course of manufacturing the fillers.

#### ACKNOWLEDGMENTS

The work is part of a project funded by King Abdulaziz University in Saudi Arabia (contract grant number MB/11/12/436). The authors acknowledge their technical and financial support.

#### REFERENCES

1. Mottahed, B. D.; Manoochehri, S. *Polym.-Plast. Technol. Eng.* **1995**, *34*, 271.
2. Lakshmi, K.; John, H.; Mathew, K. T.; Joseph, R.; George, K. E. *Acta Mater.* **2009**, *57*, 371.
3. Kaynak, A.; Polat, A.; Yilmazer, U. *Mater. Res. Bull.* **1996**, *31*, 1195.
4. Lu, G.; Li, X.; Jiang, H. *Compos. Sci. Technol.* **1996**, *56*, 193.
5. Rahaman, M.; Chaki, T. K.; Khastgir, D. *J. Mater. Sci.* **2011**, *46*, 3989.
6. Chung, D. D. L. *Carbon* **2001**, *39*, 279.
7. Chiang, W.-Y.; Cheng, K.-Y. *Polym. Compos.* **1997**, *18*, 748.
8. Al-Hartomy, O. A.; Al-Ghamdi, A. A.; Al-Salamy, F.; Dishovsky, N.; Shtarkova, R.; Slavcheva, D.; Iliev, V.; El-Tantawy, F. *Polym.-Plast. Technol. Eng.* **2013**, *52*, 1113.
9. Al-Hartomy, O. A.; Al-Ghamdi, A. A.; Al-Salamy, F.; Dishovsky, N.; Slavcheva, D.; Iliev, V.; El-Tantawy, F. *Fullerenes Nanotubes Carbon Nanostruct.* **2013**, *22*, 332.
10. Feng, Y.; Qiu, T.; Li, X.; Shen, C. *J. Wuhan Univ. Technol. Mater. Sci. Ed.* **2007**, *22*, 266.
11. Dishovsky, N. *J. Univ. Chem. Technol. Metall.* **2009**, *44*, 115.
12. Al-Ghamdi, A. A.; Al-Hartomy, O. A.; Al-Salamy, F. R.; Dishovsky, N.; Malinova, P.; Lakov, L. *Proc. Inst. Mech. Eng. Part L*, **2015**, doi: 10.1177/1464420715602141.
13. Cao, M.-S.; Song, W.-L.; Hou, Z.-L.; Wen, B.; Yuan, J. *Carbon* **2010**, *48*, 788.
14. Wen, B.; Cao, M.-S.; Hou, Z.-L.; Song, W.-L.; Zhang, L.; Lu, M.-M.; Jin, H.-B.; Fang, X.-Y.; Wang, W.-Z.; Yuan, J. *Carbon* **2013**, *65*, 124.
15. Jana, P. B.; Mallick, K.; De, S. K. *IEEE Trans. Electromagn. Compatibility* **1992**, *34*, 478.
16. Paul, C. R. *Introduction to Electromagnetic Compatibility*; Wiley: Hoboken, NJ, **2006**.
17. Ott, H. W. *Electromagnetic Compatibility Engineering*; Wiley: Hoboken, NJ, **2009**.
18. Hernandez, B. Graduate School of Clemson University, Ph. D. Dissertation, South Carolina, **2013**.
19. Graphene-Based Polymer Nanocomposites in Electronics; Sadasivuni, K. K., Ponnamma, D., Kim, J., Thomas, S., Eds.; Springer: Cham, Switzerland: **2015**.
20. Sung-Hoon, P.; Theilmann, P. T.; Asbeck, P. M.; Bandaru, P. R. *IEEE Trans. Nanotechnol.* **2010**, *9*, 464.
21. Hong, Y. K.; Lee, C. Y.; Jeong, C. K.; Lee, D. E.; Kim, K.; Joo, J. *Rev. Sci. Instrum.* **2003**, *74*, 1098.
22. Więckowski, T. W.; Janukiewicz, J. M. *Fibres Text. East. Eur.* **2006**, *14*, 18.
23. Chen, L. F.; Ong, C. K.; Neo, C. P.; Varadan, V. V.; Varadan, V. K. *Microwave Electronics: Measurement and Materials Characterization*; Wiley: Chichester, United Kingdom, **2004**.
24. Puryanti, D.; Ahmad, S. H.; Abdullah, M. H. *Polym.-Plast. Technol. Eng.* **2006**, *45*, 561.
25. Al-Hartomy, O.; Al-Ghamdi, A.; Al-Salamy, F.; Dishovsky, N.; Mihaylov, M.; Ivanov, M.; El-Tantawy, F. *J. Polym. Res.* **2012**, *19*, 1.
26. Al-Hartomy, O. A.; Al-Salamy, F.; Al-Ghamdi, A.; Dishovsky, N.; Ivanov, M.; Mihaylov, M.; El-Tantawy, F. *Int. J. Polym. Sci.* **2011**, *2011*, 8.